

UC Berkeley

UC Berkeley Previously Published Works

Title

Caspase-6-cleaved tau is relevant in Alzheimer's disease and marginal in four-repeat tauopathies: Diagnostic and therapeutic implications

Permalink

<https://escholarship.org/uc/item/0zt1h02c>

Journal

Neuropathology and Applied Neurobiology, 48(5)

ISSN

0305-1846

Authors

Theofilas, Panos
Piergies, Antonia MH
Oh, Ian
et al.

Publication Date





2022-08-01

DOI

10.1111/nan.12819

Peer reviewed

Caspase-6-cleaved tau is relevant in Alzheimer's disease and marginal in four-repeat tauopathies: Diagnostic and therapeutic implications

Panos Theofilas¹  | Antonia M. H. Piergies¹ | Ian Oh¹ | Yoo Bin Lee¹ | Song Hua Li¹ | Felipe L. Pereira¹ | Cathrine Petersen¹ | Alexander J. Ehrenberg¹  | Rana A. Eser¹ | Andrew J. Ambrose² | Brian Chin³ | Teddy Yang³ | Shireen Khan⁴ | Raymond Ng⁴ | Salvatore Spina¹ | William W. Seeley^{1,5} | Bruce L. Miller^{1,6} | Michelle R. Arkin²  | Lea T. Grinberg^{1,5,6,7} 

¹Memory and Aging Center, UCSF Weill Institute for Neurosciences, University of California San Francisco, San Francisco, California, USA

²Department of Pharmaceutical Chemistry and Small Molecule Discovery Center, University of California San Francisco, San Francisco, California, USA

³Shanghai ChemPartner, Shanghai, China

⁴ChemPartner San Francisco, South San Francisco, California, USA

⁵Department of Pathology, University of California San Francisco, San Francisco, California, USA

⁶Global Brain Health Institute, University of California San Francisco, San Francisco, California, USA

⁷Department of Pathology, University of São Paulo Medical School, São Paulo, Brazil

Correspondence

Lea T. Grinberg, John Douglas French
Alzheimer's Foundation, Neurology and
Pathology, University of California San
Francisco, 675 Nelson Rising Lane, 211B, PO
Box 1207, San Francisco, CA 94158, USA.
Email: lea.grinberg@ucsf.edu

Michelle R. Arkin, Pharmaceutical Chemistry;
Small Molecule Discovery Center, School of
Pharmacy, University of California San
Francisco, PO Box 2552; 1700 4th Street, San
Francisco, CA 94143, USA.
Email: michelle.arkin@ucsf.edu

Funding information

Alzheimer's Association, Grant/Award
Number: AARG-16-441514; National
Institutes of Health, Grant/Award Numbers:
P01AG019724, P30AG062422,
K08AG052648, U54 NS100717,
R56AG057528, K24AG053435,
K01AG053433; ShangPharma Innovation;
Rainwater Charitable Foundation

Abstract

Aim: Tau truncation (tr-tau) by active caspase-6 (aCasp-6) generates tau fragments that may be toxic. Yet the relationship between aCasp-6, different forms of tr-tau and hyperphosphorylated tau (p-tau) accumulation in human brains with Alzheimer's disease (AD) and other tauopathies remains unclear.

Methods: We generated two neopeptide monoclonal antibodies against tr-tau sites (D402 and D13) targeted by aCasp-6. Then, we used five-plex immunofluorescence to quantify the neuronal and astroglial burden of aCasp-6, tr-tau, p-tau and their co-occurrence in healthy controls, AD and primary tauopathies.

Results: Casp-6 activation was strongest in AD and Pick's disease (PiD) but almost absent in 4-repeat (4R) tauopathies. In neurons, the tr-tau burden was much more abundant in AD and PiD than in 4R tauopathies and disproportionately higher when normalising by p-tau pathology. Tr-tau astroglial pathology was detected in low numbers in 4R tauopathies. Unexpectedly, about half of tr-tau positive neurons in AD and PiD lacked p-tau aggregates, a finding we confirmed using several p-tau antibodies.

Conclusions: Early modulation of aCasp-6 to reduce tr-tau pathology is a promising therapeutic strategy for AD and PiD but is unlikely to benefit 4R tauopathies. The large percentage of tr-tau-positive neurons lacking p-tau suggests that many vulnerable neurons to tau pathology go undetected when using conventional p-tau antibodies. Therapeutic strategies against tr-tau pathology could be necessary to modulate the extent of tau

Panos Theofilas and Antonia M.H. Piergies are co-first author. Michelle R. Arkin and Lea T. Grinberg are co-senior author.

abnormalities in AD. The disproportionately higher burden of tr-tau in AD and PiD supports the development of biofluid biomarkers against tr-tau to detect AD and PiD and differentiate them from 4R tauopathies at a patient level.

KEYWORDS

Alzheimer's disease, caspase-6, cell counting, immunohistochemistry, tau cleavage, tau hyperphosphorylation, tau isoforms, tauopathies

INTRODUCTION

Tau post-translational modifications (PTMs) define and modulate tau function in healthy and diseased states. Tauopathies, a major group of neurodegenerative diseases including Alzheimer's disease (AD), Pick's disease (PiD), corticobasal degeneration (CBD), progressive supranuclear palsy (PSP) and argyrophilic grain disease (AGD), share a progressive accumulation of pathological tau in the brain [1–3]. Although tauopathies are classically defined by the morphology and distribution of phosphorylated tau (p-tau) aggregates, other underexplored tau PTMs are also critical to tau pathogenesis [4–6].

Proteolytic truncation of tau (tr-tau) by active caspases has recently been recognised as a significant contributor to tau-driven nosology in AD and primary tauopathies [7–10]. Caspases (Casp), cysteine-aspartic proteases, are proteolytic enzymes with well-defined roles in apoptosis and inflammation that cleave their substrates after specific aspartic acid (D) residues [11,12]. Effector caspases, including Casps-3 and Casps-7, and Casp-6, promote apoptosis by processing multiple structural and regulatory proteins critical for cell survival and maintenance when activated. In addition to being an executioner of apoptosis, active caspase-6 (aCasp-6) can also act as a non-apoptotic caspase and contribute to synaptic pruning during development and inflammation [11,13,14]. aCasp-6 is found to cleave tau at confirmed and putative sites, such as Asp (D) 421 (D421)—a C-terminal site contributing to tau aggregation and the formation of tau neurofibrillary tangles (NFTs) [7,9]. In this context, previous studies, ours included, demonstrated relatively high levels of aCasp-6 in the AD brain that co-occurs with an increasing burden of AD-associated abnormal proteins, such as the amyloid-beta peptide and phospho-tau [15–17]. In our study, we detected increased levels of aCasp-6 positive neurons in cases in progressive AD neuropathological stages [17]. Such increase of aCasp-6 positive neurons correlated with higher numbers of phosphorylated tau (Ser 202 [CP13]) positive neurons. This early and progressive increase of aCasp-6 levels in AD corroborates the hypothesis that caspase-6 activation exerts other roles beyond executing the last steps of the apoptotic process. Thus, modulation of Casp-6 activation may minimise pathological tau cleavage, representing a promising therapeutic strategy in AD. However, fundamental gaps in our understanding of the relationship between aCasp-6, tr-tau and p-tau deposits in human neurons and astroglia persist. For example, it is unclear whether aCasp-6 is detected in other tauopathies in addition to AD. Moreover, our knowledge on tr-tau burden in tauopathies and the extent to which tr-tau and p-tau aggregates co-occur in the same cells is practically limited to AD

Key points

- Tau truncation (tr-tau) by active caspase-6 (aCasp-6) generates toxic tau fragments prone to self-aggregation.
- The study generated two neopeptide monoclonal antibodies against tr-tau sites (D402 and D13) targeted by aCasp-6.
- The study used 5-plex immunofluorescence to quantify presence and co-occurrence of aCasp-6, tr-tau, and p-tau in neurons and astroglia in healthy controls, AD, and primary tauopathies.
- Neurons in AD and Pick's disease (PiD) showed high Casp-6 activation and disproportionately high levels of tr-tau.
- A significant subpopulation of tr-tau positive neurons lacks p-tau signal.

among all tauopathies and focused on D421. Other caspases cleave D421, and aCasp-6 cleaves other putative tau sites, including D402 near the C-terminus and D13 near the N-terminus of tau [16,18,19]. In AD, D402 tr-tau levels (detected by polyclonal antibodies) in NFTs and neuropil threads were associated with lower global cognitive scores in cases with no history of cognitive impairment, suggesting that tau truncation may be an early event in AD pathogenesis [15]. Additionally, levels of D402 tr-tau correlate with pathological p-tau and neuronal loss in human brains affected by AD [16,18], and it has been tested as a CSF biomarker for AD since its levels positively correlate with AD severity [20]. In vitro studies have also shown that tau cleavage by aCasp-6 at D13, which is at the centre of the Tau-12 and 5A6 epitopes, results in the loss of immunoreactivity with both Tau-12 and 5A6 N-terminal antibodies, suggesting a role for aCasp-6 in the N-terminal truncation of tau [19]. However, more comprehensive investigation of D13 and D402 tr-tau forms in tauopathies has been limited, first by the lack of reliable monoclonal antibodies (mAbs) targeting these specific cleavage sites, second because technology enabling multiplex immunostaining has been developed only recently and third because most studies lack other tauopathies, except for AD.

To interrogate the burden of Casp-6 tr-tau in human tauopathies and generate insights on the potential relevance of therapeutic modulation of Casp-6 activity in these diseases, we generated two novel

TABLE 1 Demographic, clinical and neuropathological characteristics of the 37 cases included in the study

Clinical diagnosis	Case	Brain region	Sex	Age of death (years)	PMI	Brain weight (grams)	CDR	NIA-AA ABC scores
Alzheimers disease	1	MFG/ITG	F	64	7.3	870	3	A3, B3, C3
	2	MFG/ITG	M	59	9	1,090	3	A3, B3, C3
	3	MFG	F	67	9.7	1,001	2	A3, B3, C3
	4	MFG/ITG	M	64	6.8	1,197	3	A3, B3, C3
	5	MFG	M	71	6.5	1,029	3	A3, B3, C3
	6	MFG/ITG	F	74	9.8	1,215	3	A3, B3, C3
	7	ITG	F	75	6.9	1,006	3	A3, B3, C3
	8	MFG	M	60	6.1	912	3	A3, B3, C3
Argyrophilic grain disease	1	MFG/ITG	F	88	17.8	1,280	0.5	A1, B2, C1
	2	MFG/ITG	M	77	4.9	1,236	0.5	A1, B1, C1
	3	MFG/ITG	M	87	6.4	1,225	0	A1, B1, C0
	4	ITG	M	68	8.3	1,511	1	A0, B2, C0
Corticobasal degeneration	1	MFG/ITG	M	66	12.1	NA	0.5	A1, B1, C0
	2	MFG/ITG	F	64	8.6	1,187	0.5	A1, B1, C0
	3	MFG/ITG	M	73	8.2	1,192	3	A1, B1, C0
	4	ITG	M	79	5.7	1,414	0.5	A0, B1, C0
	5	MFG	F	64	7.8	1,132	0.5	A0, B1, C0
	6	MFG/ITG	F	64	6.1	1,157	3	A0, B1, C0
	7	ITG	F	63	5.8	1,023	1	A1, B1, C0
	8	MFG	M	63	11.9	1,152	3	A1, B1, C0
	9	MFG	M	78	24	NA	3	A1, B1, C0
	10	MFG	M	65	4.5	1,100	3	A1, B1, C0
Picks disease	1	MFG/ITG	M	64	13.7	1,017	2	A1, B0, C0
	2	MFG/ITG	F	69	6.3	1,032	3	A0, B1, C0
	3	MFG/ITG	M	57	12.4	1,113	3	A1, B1, C0
	4	ITG	M	60	15.2	927	3	A0, B0, C0
	5	MFG	F	76	5.9	929	3	A1, B0, C1
	6	ITG	M	56	9.2	990	3	A1, B1, C1
Progressive supranuclear palsy	1	MFG	F	69	18.5	1,132	0.5	A1, B1, C0
	2	MFG/ITG	M	70	13.4	1,134	0.5	A0, B1, C0
	3	ITG	M	68	10.1	1,250	0.5	A0, B0, C0
	4	MFG/ITG	F	86	5.3	1,011	1	A0, B1, C0
	5	MFG/ITG	F	68	13	1,170	0.5	A1, B0, C0
	6	MFG/ITG	M	80	7.9	1,285	2	A1, B1, C0
	7	MFG/ITG	F	73	7.1	1,183	0.5	A2, B1, C1
Control	1	MFG/ITG	M	76	8.2	1,324	0	A1, B1, C1
	2	MFG/ITG	F	86	6.4	1,300	0	A0, B1, C0

Abbreviations: NIA-AA, National Institute on Aging and Alzheimers Association; MFG, Middle Frontal Gyrus; ITG, Inferior Temporal Gyrus.

epitopes (neopeptide) mAbs targeting proteolytic sites predominantly cleaved by aCasp-6: D13 and D402. Next, we used a recently developed five-plex immunofluorescence (IF) protocol to quantify and map neurons and astroglia positive for D13 and D402 tr-tau and investigate their

relationship to aCasp-6 and p-tau (Ser 202 and Ser396/Ser404) aggregates in two cortical areas of a well-characterised post-mortem brain cohort with AD; PiD, a sporadic 3-repeat (3R); PSP, CBD and AGD, all sporadic 4-repeat (4R) tauopathies; and healthy ageing controls.

MATERIALS AND METHODS

Participants

This study was exempt from ethical approval by the University of California, San Francisco (UCSF) institutional review board. Post-mortem human brains were obtained from UCSF's Neurodegenerative Disease Brain Bank [21]. All brains underwent standardised neuropathological assessment for neurodegenerative diseases that follow universally accepted guidelines [22,23]. Inclusion criteria included a post-mortem interval under 24 h and a lack of more than one primary neuropathological diagnosis, an Axis I psychiatric disorder diagnosis, a non-dementia neurological disorder and gross non-degenerative structural neuropathology. Control cases were free of any clinical symptoms of cognitive decline and neurological or non-incident neuropathological diagnoses. To provide a broad picture of the most common sporadic tauopathies, our cohort includes AD (3R/4R), AGD (4R), CBD (4R), PiD (3R) and PSP (4R), as well as clinical and pathological age-matched controls. We used 21 cases with matching MFG and ITG regions (4 AD, 3 AGD, 4 CBD, 3 PiD, 5 PSP and 2 Controls) and 16 cases where either the MFG or ITG region was available (4 AD, 1 AGD, 6 CBD, 3 PiD and 2 PSP), totalizing 28 cases per region of interest. Table 1 summarises all 37 cases.

Development of caspase-6-cleaved tau neopeptide monoclonal antibodies

Except for TauC3 (D421), mAbs against Casp-6 tr-tau are not available. In collaboration with ChemPartner, we generated two neopeptide mAbs targeting tau cleaved by Casp-6: mAbD13 (14-442; Peptide I: HAGTYGLGDRKC) and mAbD402 (1-401; Peptide II: CIVYKSPVVS GD). Briefly, both mAbs were produced by immunising 6- to 8-week-old wild type Balb/c, and SJL mice (SLAC) with keyhole limpet hemocyanin (KLH) conjugated tau peptides using protocols approved by the ChemPartner IACUC committee. A total of 50 µg of each peptide was injected into each mouse's abdominal cavity along with 0.25 ml of Complete Freund's Adjuvant (Sigma). Blood samples were collected 1 week after immunisation. The antibody titre and specificity in serum were determined by enzyme-linked immunosorbent assay (ELISA) analysis against BSA-conjugated peptides I and II [24]. Western blot further confirmed antibody specificity against full-length tau, tau 1-402, and tau 14-441 recombinant proteins, with total tau being used to confirm equal loading [24]. Mice with specific immune responses against tau peptides were selected for fusion and were given a final boost by intraperitoneal injection of 100 µg of the corresponding immunogen. After 4 days, all mice were sacrificed, and their splenocytes lysed in NH₄OH at 1% (w/w), followed by centrifugation at 1,000 rpm and washes with DMEM (Invitrogen). Viable splenocytes were fused with mouse myeloma cells SP2/O (ATCC) at a ratio of 5:1 with high-efficiency electric fusion (BTX ECM200). Fused cells were re-suspended in DMEM with 20% FBS and hypoxanthine-aminopterin-thymidine (HAT) medium (Invitrogen). Fourteen days

after cell fusion, hybridoma supernatants were collected and screened by ELISA. Clones with an OD_{450nm} > 1.0 were expanded in a 24-well plate containing DMEM with 10% heat-inactivated FBS, and supernatants were collected after 3 days of culture. The antibody isotypes were determined, and ELISA and western blot were used to test their ability to bind to tau. Clones that showed desired reactivity and specificity against tau were subjected to subcloning to get stable monoclonal hybridoma cells. Sub-cloning was carried out by limited dilution in a 96-well plate with DMEM media containing 10% FBS. Clones with specific tau binding were further expanded in DMEM media containing 10% FBS for subsequent antibody production and cryopreservation. See Section S1 for the analysis of antibody specificity.

Tissue processing and multiplex immunofluorescence staining

We performed immunofluorescence (IF) assays on eight µm thick tissue sections from paraffin-embedded tissue blocks of the middle frontal gyrus and inferior temporal gyrus. Each single slide underwent immunohistochemical detection for up to five antibodies to detect: neurons (NeuN), p-tau (CP13/PHF-1), aCasp-6 and Casp-6-tr-tau (see Table S1 for a list of primary antibodies). Here, we chose to use CP13 and PHF-1 as a proxy for p-tau because the phosphorylation of tau at Ser 202 and Ser396/Ser404 occurs earlier in AD, is present in all tauopathies and rarely occurs in healthy brains [25,26].

As we found a significant number of tr-tau positive neurons lacking signal for CP13 in AD cases, we conducted additional experiments to probe other common p-tau sites in tauopathies, as tau cleavage by caspases could lead to loss of tau fragments containing phospho-epitopes recognised by a given p-tau antibody. First, we conducted double labelling immunostaining for mAbCP13 and one of the following p-tau monoclonal antibodies: mAbPHF-1, mAbAT100 and mAbT231 in AD cases (Table S1). We observed that practically all neurons positive for AT100 and T231 were also positive for CP13. However, about 15% of neurons positive for PHF-1 lacked CP13 positivity (Figure S3). Thus, we included an additional set of quantification in the same AD and PiD cases and areas using a combination of PHF-1, mAbD13 and mAbD402 antibodies to interrogate the proportion of neuronal overlap between PHF-1 (p-tau) and D13 and D402 tr-tau.

Multiplex IF was performed on a Ventana discovery ultra-automated staining instrument (Roche) with antibodies there were previously characterised in single labelled immunostaining. Tissue sections were initially incubated with the mAbD13 antibody (1:150) overnight, followed by the Discovery anti-mouse HQ, anti-HQ HRP and FAM kit (Roche) for signal development. mAbD13 was stripped by a denaturing solution of β-mercaptoethanol and SDS (BME/SDS; Sigma) as previously described [27]. Next, sections were incubated with NeuN (1:300) at room temperature for 1 h, followed by goat anti-guinea pig HRP (1:200, Advansta). NeuN signal was developed using the Discovery DCC kit (Roche). Excess unbound secondary HRP was removed by incubating sections in Ventana BenchMark Ultra CC2

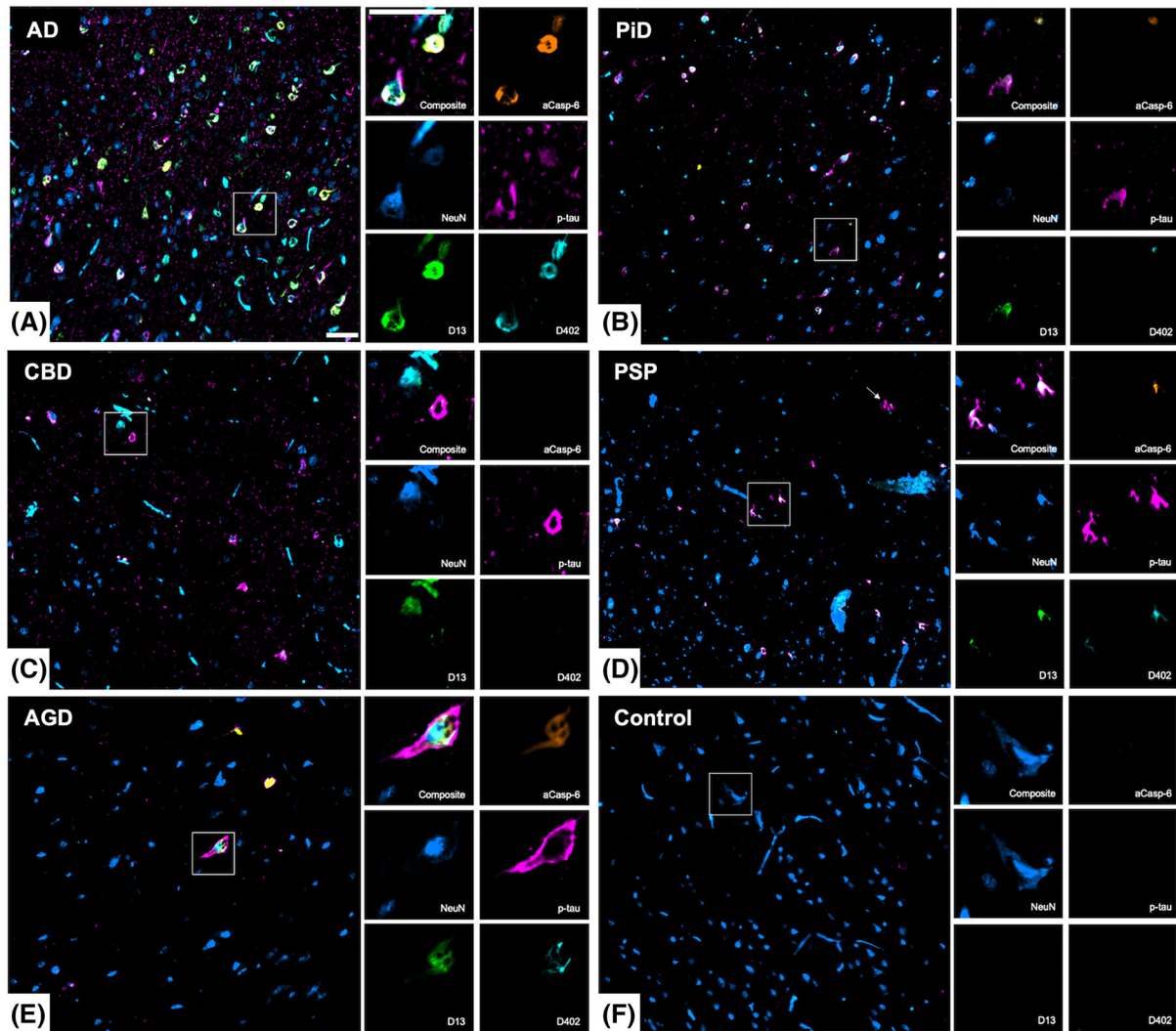


FIGURE 1 Neuronal marker positivity in the middle frontal and inferior temporal gyrus of human post-mortem brains with common tauopathies. Low and high magnification images showing multiplex immunofluorescence staining of neurons (NeuN, blue), active caspase-6 (aCasp-6, orange), neoepitope mAbs of caspase-6-cleaved tau sites (D402 and D13, green and cyan, respectively), and phosphorylated tau (Ser 202; p-tau, magenta). Compared to other tauopathies (B–E), AD (A) showed the most robust positivity for all markers, while no or negligible positivity was observed in controls (F). Abbreviations: AD, Alzheimers disease (A); PiD, picks disease (B); CBD, corticobasal degeneration (C); PSP progressive supranuclear palsy (D); AGD, argyrophilic grain disease. Scale bars: 50 μ m

solution (Roche) at 95°C for 8 min, followed by incubation with mAb CP13 (1:4,000) or PHF-1(1:12,000) at room temperature for 1 h (see Table S1 for a complete list of antibodies). CP13 signal was developed using the Discovery omnimap anti-mouse HRP and Cy5 kit (Roche). To avoid cross-reaction between CP13 and mAb402 primary antibodies, an antibody stripping step using Ventana BenchMark Ultra CC2 solution at 100°C followed by Discovery antibody denaturing reagent was performed after development of CP13. Finally, sections were incubated with the remaining primary antibodies—a cocktail of active caspase-6 (1:800) and mAbD402 (1:700)—at room temperature for 6 h. The active caspase-6 signal was developed with Discovery omnimap anti-rabbit HRP and Rhod 6G kit (Roche). mAbD402 signal was developed with biotinylated anti-mouse (1:200, Vector Laboratories) with Streptavidin Alexa Fluor 790 (1:200, Thermo Fisher). To

reduce autofluorescence, sections were incubated in 0.8% Sudan Black B (Sigma) in 70% ethanol and coverslipped with prolong anti-fade mounting media (Invitrogen). All reactions included antibody elution controls as described in Ehrenberg et al. [27].

Quantitative analysis of positive markers

Cell quantification was performed blinded to clinical and neuropathological diagnosis and independently reviewed by three of the co-authors. Each region of interest (ROI) was imaged at 20X magnification with a Zeiss Axiomager A2 microscope equipped with a Zeiss Colibri 7: Type FRR [G/Y] CBV-UC 7-channel fluorescence light source and an electronic platform. AF350 was visualised using a DAPI

filter set, AF488 with a GFP filter set, AF546 with a DsRed filter set, AF647 with a Cy5 filter set and AF790 with a Cy7 filter set. Figures 1 and 2 show representative examples of positive markers in neurons (all tauopathies) and astroglia (CBD and PSP), respectively. A semi-automated pipeline was used to quantify marker positivity in both cell types (Figure 3). This approach is further described in Section S1.

Statistical analysis

Data analysis was performed using R Statistical Software (version 3.6.1; R Foundation for Statistical Computing, Vienna, Austria). Means and standard deviations were calculated for demographic and quantitative neuropathological data. Heatmaps and Venn diagrams were created using *superheat* and *eulerr* libraries, respectively. Proportion of Neuronal positivity for mAbD402, mAbD13 and aCasp6 was compared using Mann–Whitney U test.

RESULTS

Table 1 summarises the demographic, clinical and neuropathological characteristics of all 37 cases used in this study. A total of 56.75% were male, the mean (SD) age of death was 70.02 (8.52) years, the mean (SD) post-mortem interval was 9.37 (4.28) h and the mean (SD) brain weight was 1,135.02 (144.14) g.

All tauopathies show expected positivity for neuronal p-tau

We used the p-tau mAbCP13 (Table S1) to map p-tau Ser 202-positive neurons in five sporadic tauopathies and healthy controls. All cases showed expected percentages of neuronal p-tau inclusions in the MFG and ITG. In the MFG, the minimal neuronal p-tau

positivity in AGD (an average of 0.03%) was anticipated since this region is typically spared of tau pathology. Of note, in controls, we found p-tau positivity in an average of 0.09% of ITG neurons, which is within the bounds expected in Braak stage 1/2 cases [28]. Overall, our results confirm the presence of tau lesions in predicted regions based on disease diagnosis and provide a basis for interpreting the magnitude of tr-tau burden (Table 2; Figure 4).

In AD and PiD, the proportion of neurons positive for aCasp-6 is significantly higher than in other tauopathies tested

We and others previously found higher numbers of neurons positive for aCasp-6 in AD than in controls. aCasp-6 promotes tau cleavage. Here, we investigated other common tauopathies also that show increased burden of aCasp-6 positive neurons (Table 2; Figures 4 and 5). aCasp-6 positivity was absent in controls. In AD, we found that an average of 4.23% neurons in the MFG and 6.38% of neurons in ITG were positive for aCasp-6, while in PiD, we found 4.82% and 4.9%, respectively. Conversely, the percentage of aCasp-6 positive in the other tauopathies was at most, less the 1/4 of the values found in AD and PiD (CBD, ITG). Non-parametric tests confirm that neuronal aCasp-6 is almost negligible in the 4R-tauopathies compared to AD and PiD.

Neuronal cleaved tau aggregates are also more prominent in AD and PiD than in 4-repeat tauopathies

Previous studies focusing on the tr-tau sites D421 (mAbTauC3) and D402 (polyclonal antibody) showed tr-tau aggregates in AD, but relatively little is known about tr-tau aggregates in common primary tauopathies. Here, we used neopeptide mAbs targeting tau cleaved by Casp-6 at a C-terminal site (D402) and a previously unexplored N-terminal site (D13) to quantify the magnitude of tr-tau pathology in

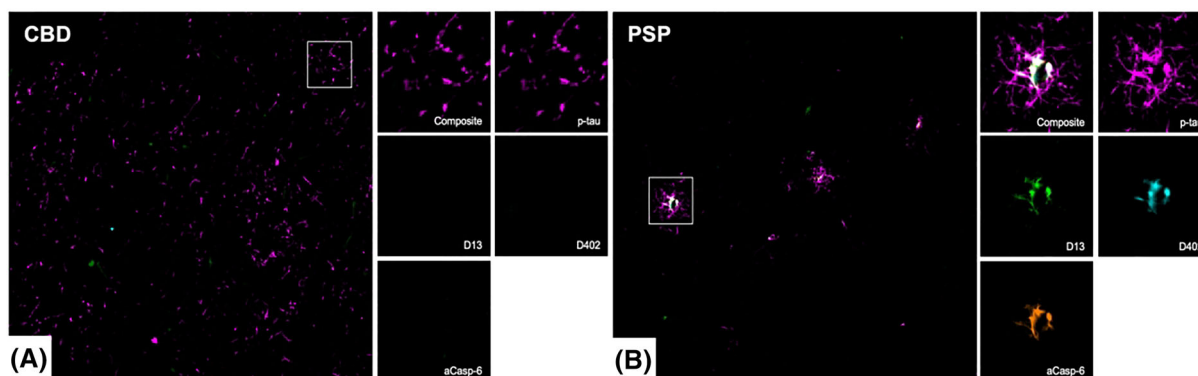
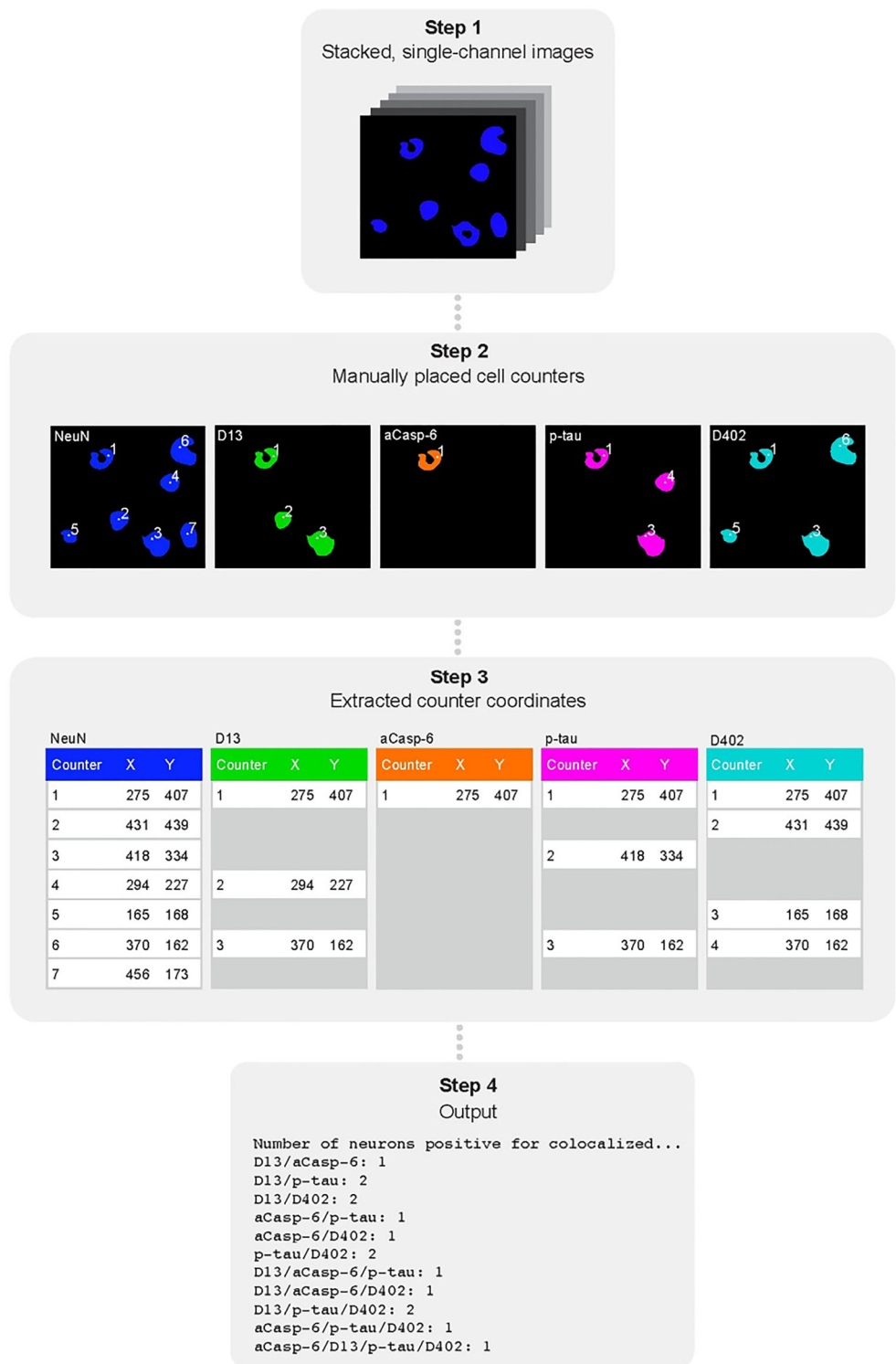


FIGURE 2 Multiplex immunofluorescence images showing the co-occurrence of phosphorylated-tau (Ser202, magenta), active caspase-6 (aCasp-6, orange) and neopeptide mAbs against caspase-6-cleaved tau sites (D402 and D13, green and cyan, respectively) in astroglial cells from human post-mortem brains affected by CBD (A) and PSP (B). PSP (B) showed greater positivity for all markers, as compared to CBD (A). Abbreviations: CBD, corticobasal degeneration (A); PSP progressive supranuclear palsy (B). Scale bars: 50 μ m

FIGURE 3 Schematic of the semi-automated cell counting approach. First, single-channel images were stacked (step one) followed by manual placement of counters on positive cells using FIJIs built-in counting tool (step two). Next, counter coordinate data were extracted from FIJI files (step three). The number and type of co-occurring markers were determined by searching for coordinates present within a two-pixel radius of each other using a Python script (step four). Abbreviations: aCasp-6, active caspase-6; p-tau, phosphorylated tau



AD and other tauopathies (Tables 2 and 3 and Figures 4 and 5). mAbD13- and mAbD402-immunoreactive deposits in neurons in all tauopathies showed neuronal cytoplasmic inclusions that were absent in healthy controls. The morphology of these inclusions resembled the ones seen with p-tau antibodies, that is, tangles in AD, Pick's bodies and neurons in PiD (Figures 1 and S2). Glia pathology in PSP and CBD resembled tufted astrocytes and astrocytic plaques, respectively (Figure 2). Overall, neuronal positivity for mAbD402 in ITG was at

least six times greater in AD and PiD than in other tauopathies, reaching as much as 6.66% on MFG neurons and 6.08% of ITG neurons in AD (Table 2; Figure 4). Curiously, the proportion of D402 positive neurons in PiD was much smaller in MFT than in ITG. The proportion of mAbD402 positive neurons in AD was statistically significantly higher in AD than all 4R-tauopathies in both areas and of PiD in MFG (Table 3). The neuronal burden of D13 tr-tau was also significantly higher in AD and PiD than in other 4R-tauopathies

TABLE 2 Mean (SD) percentage of neurons positive for the active caspase-6, D402 truncated tau, D13 truncated tau, phosphorylated tau, individually and in combination

Variable	Middle frontal gyrus						Inferior temporal gyrus	
	AD	AGD	CBD	PiD	PSP	Control	AD	5
n	7	3	8	4	6	2	AD	5
Number of neurons (NeuN)	1,033.43 (250.21)	1,297.00 (221.47)	1,143.88 (211.39)	1,227.50 (448.56)	1,037.00 (231.61)	862.00 (446.89)	1,339.40 (412.70)	
Neuronal aCasp-6 (%)	4.23 (2.62)	0.00 (0.00)	0.22 (0.42)	4.82 (4.98)	0.54 (0.92)	0.00 (0.00)	6.38 (3.43)	
Neuronal p-tau (CP13) (%)	5.59 (2.48)	0.03 (0.00)	3.73 (2.38)	11.58 (6.85)	1.15 (0.66)	0.00 (0.00)	7.24 (5.40)	
Neuronal D402 tr-tau (%)	6.66 (4.40)	0.00 (0.00)	0.06 (0.10)	1.57 (1.80)	0.18 (0.34)	0.00 (0.00)	6.08 (4.11)	
Neuronal D13 tr-tau (%)	4.70 (2.17)	0.00 (0.00)	1.62 (2.59)	6.01 (3.69)	0.61 (0.60)	0.18 (0.26)	6.52 (3.22)	
aCasp-6 + p-tau (%)	1.11 (0.82)	0.00 (0.00)	0.03 (0.05)	3.31 (3.65)	0.14 (0.20)	0.00 (0.00)	2.64 (1.60)	
aCasp-6 + D402 tr-tau (%)	3.31 (2.69)	0.00 (0.00)	0.00 (0.00)	1.49 (1.73)	0.00 (0.00)	0.00 (0.00)	3.81 (1.97)	
aCasp-6 + D13 tr-tau (%)	1.73 (1.68)	0.00 (0.00)	0.08 (0.15)	3.04 (2.84)	0.04 (0.07)	0.00 (0.00)	4.10 (2.65)	
D402 tr-tau + p-tau (%)	1.72 (1.10)	0.00 (0.00)	0.00 (0.00)	0.92 (1.12)	0.10 (0.20)	0.00 (0.00)	1.87 (1.46)	
D13 tr-tau + p-tau (%)	2.66 (1.47)	0.00 (0.00)	0.43 (0.33)	3.89 (3.00)	0.31 (0.46)	0.00 (0.00)	3.09 (1.72)	
D402 tr-tau + D13 tr-tau (%)	2.30 (1.28)	0.00 (0.00)	0.00 (0.00)	1.17 (1.35)	0.08 (0.15)	0.00 (0.00)	2.87 (1.76)	
aCasp-6 + D402 tr-tau + p-tau (%)	0.75 (0.67)	0.00 (0.00)	0.00 (0.00)	0.87 (1.07)	0.00 (0.00)	0.00 (0.00)	1.49 (1.05)	
aCasp-6 + D13 tr-tau + p-tau (%)	0.90 (0.76)	0.00 (0.00)	0.02 (0.05)	2.33 (2.43)	0.03 (0.04)	0.00 (0.00)	2.25 (1.38)	
aCasp-6 + D402 tr-tau + D13 tr-tau (%)	1.33 (1.33)	0.00 (0.00)	0.00 (0.00)	1.14 (1.32)	0.00 (0.00)	0.00 (0.00)	2.59 (1.75)	
D402 tr-tau + D13 tr-tau + p-tau (%)	1.38 (0.86)	0.00 (0.00)	0.00 (0.00)	0.80 (1.01)	0.06 (0.10)	0.00 (0.00)	1.57 (1.20)	
aCasp-6 + D402 tr-tau + D13 tr-tau + p-tau (%)	0.63 (0.51)	0.00 (0.00)	0.00 (0.00)	0.77 (0.97)	0.00 (0.00)	0.00 (0.00)	1.43 (1.07)	

Note: All cases showed expected neuronal p-tau positivity, based on their diagnosis. AD and PiD cases showed the strongest positivity for neuronal caspase-6. AD and PiD cases showed the highest percentage of neurons positive for mAbsD402 and mAbsD13. Numbers for individual markers include neurons that are positive for more than one marker. Abbreviations: aCasp-6, active caspase-6; AD, Alzheimer's disease; AGD, argyrophilic grain disease; CBD, corticobasal degeneration; PiD, Pick's disease; PSP, progressive supranuclear palsy; p-tau, phosphorylated tau.

TABLE 2 (Continued)

Variable	Inferior temporal gyrus				
	AGD	CBD	PiD	PSP	Control
n	4	6	5	6	2
Number of neurons (NeuN)	1,209.00 (406.88)	1,111.33 (268.83)	1,115.60 (107.53)	1,038.83 (270.13)	1,148.50 (142.13)
Neuronal aCasp-6 (%)	0.25 (0.37)	1.05 (1.42)	4.90 (3.37)	0.53 (1.01)	0.00 (0.00)
Neuronal p-tau (CP13) (%)	0.97 (0.89)	3.62 (2.11)	16.50 (10.64)	0.47 (0.31)	0.09 (0.01)
Neuronal D402 tr-tau (%)	0.24 (0.35)	0.96 (1.38)	6.63 (10.11)	0.76 (1.18)	0.04 (0.06)
Neuronal D13 tr-tau (%)	0.28 (0.34)	0.56 (0.43)	10.13 (11.17)	1.95 (3.65)	0.00 (0.00)
aCasp-6 + p-tau (%)	0.25 (0.37)	0.23 (0.33)	2.39 (1.34)	0.11 (0.10)	0.00 (0.00)
aCasp-6 + D402 tr-tau (%)	0.17 (0.22)	0.04 (0.09)	2.33 (2.49)	0.12 (0.27)	0.00 (0.00)
aCasp-6 + D13 tr-tau (%)	0.21 (0.29)	0.08 (0.19)	2.55 (2.36)	0.06 (0.09)	0.00 (0.00)
D402 tr-tau + p-tau (%)	0.18 (0.24)	0.03 (0.05)	3.36 (4.79)	0.04 (0.07)	0.00 (0.00)
D13 tr-tau + p-tau (%)	0.28 (0.34)	0.27 (0.26)	4.48 (4.18)	0.07 (0.09)	0.00 (0.00)
D402 tr-tau + D13 tr-tau (%)	0.15 (0.19)	0.01 (0.03)	4.75 (8.16)	0.13 (0.32)	0.00 (0.00)
aCasp-6 + D402 tr-tau + p-tau (%)	0.17 (0.22)	0.00 (0.00)	1.23 (1.31)	0.03 (0.05)	0.00 (0.00)
aCasp-6 + D13 tr-tau + p-tau (%)	0.21 (0.29)	0.08 (0.19)	1.38 (1.10)	0.04 (0.09)	0.00 (0.00)
aCasp-6 + D402 tr-tau + D13 (%)	0.15 (0.19)	0.00 (0.00)	1.59 (2.07)	0.02 (0.05)	0.00 (0.00)
D402 tr-tau + D13 tr-tau + p-tau (%)	0.15 (0.19)	0.01 (0.03)	2.27 (3.73)	0.02 (0.05)	0.00 (0.00)
aCasp-6 + D402 tr-tau + D13 tr-tau + p-tau (%)	0.15 (0.19)	0.00 (0.00)	0.86 (1.10)	0.02 (0.05)	0.00 (0.00)

Note: All cases showed expected neuronal p-tau positivity, based on their diagnosis. AD and PiD cases showed the strongest positivity for neuronal caspase-6. AD and PiD cases showed the highest percentage of neurons positive for mAbsD402 and mAbsD13. Numbers for individual markers include neurons that are positive for more than one marker. Abbreviations: aCasp-6, active caspase-6; AD, Alzheimers disease; AGD, argyrophilic grain disease; CBD, corticobasal degeneration; PiD, pickers disease; PSP, progressive supranuclear palsy; p-tau, phosphorylated tau.

TABLE 3 P values for the comparison of the proportion of neurons positive for active caspase-6 (top), D402 tr-tau (middle) and D13 tr-tau (bottom) among different tauopathies, per brain area using Mann–Whitney Wilcoxon tests

	AD		AGD		CBD		PiD	
	MFG	ITG	MFG	ITG	MFG	ITG	MFG	ITG
aCasp6								
AGD	0.021*	0.0195*	-	-	-	-	-	-
CBD	0.0012*	0.0087*	0.299	0.45	-	-	-	-
PiD	0.9273	0.5476	0.0436*	0.0195*	0.0277*	0.0519	-	-
PSP	0.0023*	0.0087*	0.0591	0.7461	0.2824	0.4225	0.1714	0.0173*
D402								
AGD	0.021*	0.019*	-	-	-	-	-	-
CBD	0.0012*	0.035*	0.299	0.582	-	-	-	-
PiD	0.0424*	0.548	0.1187	0.065	0.2044	0.12	-	-
PSP	0.0051*	0.022*	0.2198	0.741	0.5674	0.935	0.3789	0.035*
D13								
AGD	0.021*	0.0195*	-	-	-	-	-	-
CBD	0.0205*	0.0043*	0.0178*	0.3314	-	-	-	-
PiD	0.3152	1	0.0436*	0.0195*	0.1091	0.0043*	-	-
PSP	0.0047*	0.0519	0.0591	0.5895	0.4908	0.8726	0.0667*	0.0519

Abbreviations: aCasp-6, active caspase-6; AD, Alzheimers disease; AGD, argyrophilic grain disease; CBD, corticobasal degeneration; PiD, Picks disease; PSP, progressive supranuclear palsy.

*Statistical significance at $p < 0.05$.

opposite direction, as only 50.7–65.9% (mAbD402) and 43.1–67.9% (mAbD13) of tr-tau neurons were also positive for aCasp-6 in AD; similarly, tr-tau neurons were positive for aCasp-6 in 34.8–100% (mAbD402) and 25–51.6% (mAbD13) in PiD (Table 2; Figures 4 and 5).

In AD, a substantial percentage of neurons with tr-tau lack p-tau inclusions

Here, we evaluated the degree of co-occurrence between p-tau (Ser202) and tr-tau at D402 and D13 cleavage sites (Table 2; Figures 4 and 5). Since the percentage of neurons with D402 and D13 tr-tau was minimal in the tested 4R tauopathies (AGD, CBD and PSP), we only included AD and PiD in the analysis. In PiD, 60% and 62.9% of MFG neurons positive for D402 and D13 tr-tau, respectively, also showed p-tau (Ser202) positivity. The overlap was about 1/3 less in ITG neurons (40.9% and 44.2%). Surprisingly, only 23.2% and 26.8% of the MFG and ITG mAbD402-positive neurons showed p-tau (Ser202) positivity in AD. Overlap for D13 tr-tau and p-tau (Ser202) occurred in 56.9% and 46.4% of MFG and ITG D13-positive neurons, respectively (Table 2; Figures 4 and 5). Interestingly, D402 and D13 tr-tau only show partial neuronal co-occurrence in both diseases (Figure 5). p-tau inclusions are a hallmark of all tauopathies. Although abnormal tau phosphorylation at Ser202 is considered one of the earliest and most universal events in tau pathogenesis, other pathological p-tau species are common in tauopathies. We interrogated the possibility that another commonly used p-tau antibody could have better

overlap with tr-tau signal in the same neurons. We did further analysis using additional p-tau markers, including PHF-1 (Ser 396/ Ser 404), AT100 (Thr 212/Ser 214) and T231 (Thr231; Table S1). First, we conducted double IF staining for CP13/PHF-1, CP13/AT100 and CP13/T231 and analysed the overlap between each antibody combination. We observed that 100% of AT100 and T231 stained neurons were also positive for CP13 (Figure S3). However, the overlap between PHF-1 and CP13 was partial, with approximately 10% of the neurons positive for PHF-1, but not for CP13 (Figure S3). Considering these findings, we further probed AD and PiD cases using multiplex IF for the antibody combination PHF-1/ mAbD13/mAbD402. Overlap remained partial. Only 25.4–27.9% (mAbD402; MFG, ITG) and 47.4–38.5% (mAbD13; MFG, ITG) of tr-tau neurons were also positive for PHF-1 in AD, while 28.1–55.6% (mAbD402) and 27.6–54.2% (mAbD13) overlapped in PiD (Table S2; Figure 6).

Altogether, our results suggest that a substantial population of neurons undergoes pathological-tau changes that are not identified by p-tau, as demonstrated here using several p-tau antibodies.

Astroglial Casp-6-cleaved tau inclusions in CBD and PSP

Tau deposits in astroglia are a prominent feature of CBD and PSP [29]. Previous studies suggest that there is D421 tr-tau astroglial pathology [8] but it is less clear if D13 and D402 tr-tau also

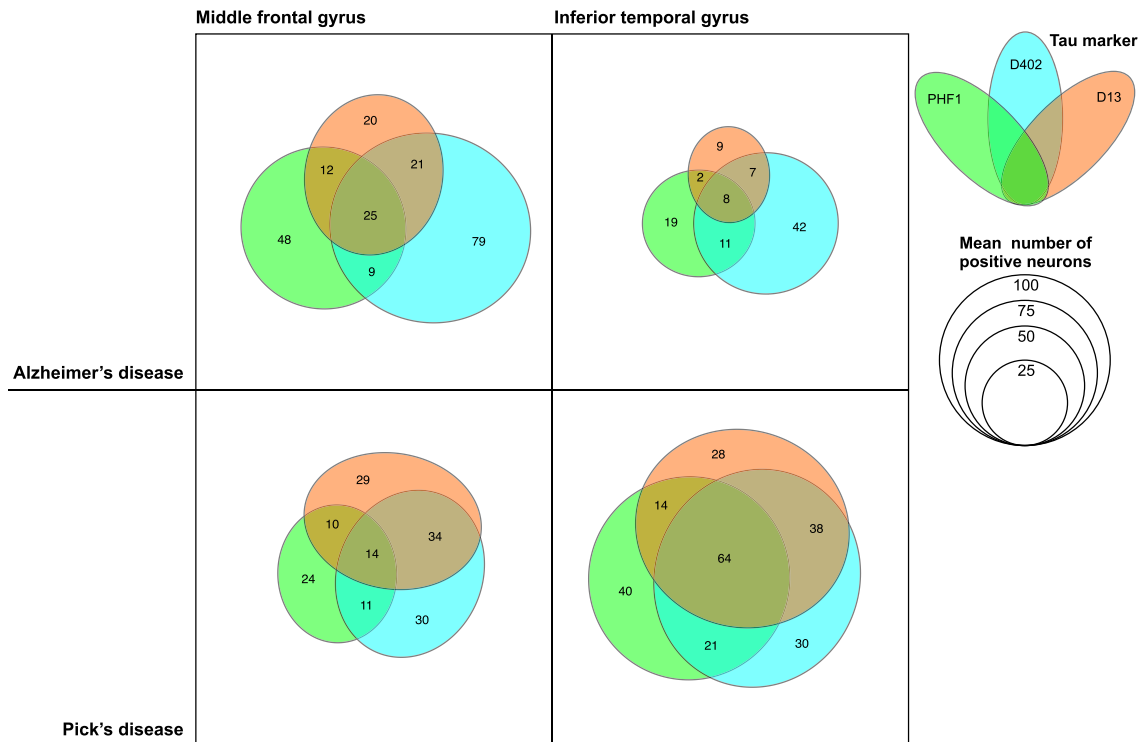


FIGURE 6 Venn diagrams illustrating the frequency of marker co-occurrence for AD and PiD, the two tauopathies with the highest marker positivity. Each coloured ellipse represents mean numbers of positive neurons for each antibody, including phosphorylated tau Ser396/404, mAbPHF-1 (green), mAbD402 (cyan) and mAbD13 (orange) identified by multiplex immunofluorescence. Abbreviations: AD, Alzheimers disease; PiD, picks disease; aCasp-6; active caspase-6; p-tau, phosphorylated tau

accumulate in astroglia as well. Here, we focused on p-tau (Ser202)-positive astroglia in CBD and PSP, since these tauopathies show dominant tau lesions in this cell type. We used tissue sections that were used to quantify tau pathological changes in neurons. PSP showed a relatively strong p-tau positivity in tufted and thorned astrocytes in the MFG and ITG (Table S3; Figures 2 and 7). In CBD, p-tau positivity in astrocytic plaques was also strong. In the MFG, 8.99% of p-tau-positive astrocytes also showed Casp-6 activity in PSP (3.70% in CBD). Overall, the percentages of p-tau positive astroglia with overlapping tr-tau were higher in PSP than in CBD, and D13 tr-tau was more prevalent than D402 tr-tau in both brain regions (Table S2). We failed to observe astroglia with tr-tau inclusions lacking p-tau. Our results suggest that astroglia, similar to neurons, show Casp-6-cleaved D13 and D402 tr-tau.

DISCUSSION

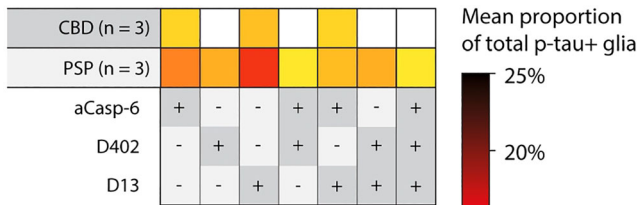
We used a recently developed five-plex immunofluorescence (IF) protocol [27], novel tr-tau mAbs and quantitative analyses to analyse two cortical areas in post-mortem brain sections from individuals with common tauopathies and healthy controls to interrogate: (1) the extent of neuronal caspase-6 activation in non-AD tauopathies; (2) the neuronal and glial burden of Casp-6-tr-tau, other than D421, in AD and other tauopathies; and (3) the frequency of co-occurrence of

N- and C-terminus tr-tau fragments, p-tau and aCasp-6 within the same neurons and astroglia. This study offers several novel findings informing mechanisms and possible strategies for diagnosing and treating AD and other tauopathies.

First, the amount of aCasp-6- and tr-tau-positive neurons burden was much higher in AD and to a lesser extent in PiD than in 4R tauopathies. In fact, evidence of Casp-6 activation was almost absent in pure 4R tauopathies (Tables 2 and S3 and Figures 4 and 7). aCasp6 mediates the truncation of tau into fragments that may be toxic and prone to self-aggregation [9,16]. Thus, it is not surprising that compared to the 4R tauopathies, the mean percentages of neurons with D402 and/or D13 tr-tau were 23.3-(D13; compared to AGD in ITG) to 111-fold higher (D402; compared to CBD in MFG) in AD. We previously showed that aCasp-6 inhibitors ameliorate tau pathology in iPSC-derived neurons with the frontotemporal dementia-causing V337M MAPT mutation [17]. Therefore, Casp inhibitors could be a promising therapy for tauopathies with significant 3R tau pathological forms, but they are unlikely to be useful in treating 4R tauopathies.

Second, the higher amount of tr-tau in AD and PiD compared to 4R tauopathies cannot be credited only to a higher number of p-tau neurons in the former. For instance, whereas the percentage of p-tau (Ser202)-positive neurons in AD was 4.86 times greater than in PSP (MFG), the percentage of tr-tau-positive neurons (mAbD402 and mAbD13) in AD were 37 and 7.7 times greater than that in PSP (MFG) and even greater than in CBD.

(A) Middle frontal gyrus



(B) Inferior temporal gyrus

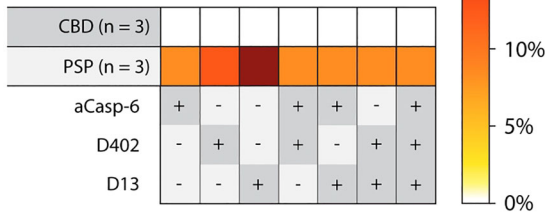


FIGURE 7 Heatmaps illustrating mean percentages of phospho-tau positive astroglia, in the middle frontal (A) and inferior temporal gyrus (B) of CBD and PSP brains, which were also positive for active caspase-6, mAbD402 and mAbD13 antibodies. CBD and PSP were selected for this analysis because they contain the greatest amount of astroglia pathology. PSP showed higher astroglia positivity for all markers, relative to CBD. Abbreviations: CBD, corticobasal degeneration; PSP, progressive supranuclear palsy. Rows represent tauopathies, controls, and a list of antibodies included in the analysis. Cells represent mean percentages of total neurons (colour gradient) found positive for individual or multiple antibodies. The +/- symbols represent the presence (+, dark grey) or absence (-, light grey) of antibody signal

The disproportionately higher burden of tr-tau relative to p-tau in AD and PiD compared to 4R tauopathies suggests that fluid-based biomarkers based on tr-tau may be superior to p-tau biomarkers with regards to AD and PiD diagnosis and efforts to differentiate these diseases from other tauopathies [30]. Developing biomarkers to detect D13 and/or D402 tr-tau is attractive and feasible. Although CSF lacks C-terminus tau peptides, making it challenging to detect tau fragments above residue 268 (e.g., D421) [31,32], our multiplex IF approach enabled us to establish that an N-terminus form of tr-tau (D13) is more abundant in neurons as compared to a C-terminus form (D402). However, mAbD13 and mAbD402 exhibit a high degree of co-occurrence. Recent studies on fluid-based biomarkers with an N-terminal assay (NT1)—including the N-terminal mAbTau12 (amino acids 6–13)—show that as NT1 levels increase, clinical decline in subjects with positivity for other AD biomarkers worsens. NT1 levels probably remain intact in non-AD dementia [33–35]. Supported by our quantitative neuropathological results and the success of other N-terminal truncated assays, mAbD13 may become an essential player in the arsenal of biofluid biomarkers against AD.

Third, and most intriguing, in AD and PiD, a subpopulation of neurons as large as the subpopulation of p-tau neurons harbours tr-tau inclusions in the absence of p-tau signal. We confirmed these findings using several p-tau antibodies (Ser 202, Ser 396/Ser 404, Thr 212/Ser 214 and Thr 231) to avoid bias in our analysis by focusing only on a single antibody. P-tau aggregates are a critical feature of all tauopathies, and most neuropathology labs rely on p-tau inclusions to

classify and stage tauopathies in humans and experimental models. Experimentally, tau cleavage at D421 causes loss of adjacent p-tau epitope S422 [36] and attenuates phosphorylation at Ser396/404 and Th231 [37]. Thus, a neurofibrillary tangle previously containing p-tau could lose p-tau epitopes as the tangle matures. Even if this would explain the great number of tr-tau+ neurons lacking p-tau signal, the results are still very relevant because this significant tau pathology is not being detected in neuropathological assessments. Evidence shows that tr-tau can independently affect neuronal function [20]. Another possibility is that neurons accumulating tr-tau may follow a pathogenic pathway independent of tau phosphorylation. Experimental and post-mortem human studies support this hypothesis by demonstrating that tr-tau is an early event leading to filament formation in tauopathies [9,36,38–40]. For instance, Horowitz et al. [19] detected N-terminal tau truncation, preceding C-terminal truncation and phosphorylation at th18 in AD. Even if these authors did not have access to an antibody specific to D13 tr-tau as we have, their results support the same conclusions. Very few studies examined the co-occurrence of neuronal tr-tau and p-tau in tauopathies. These studies used fewer cases and reported that p-tau positive neurons may or not have co-occurring tr-tau signal, not the opposite. But these studies focused on D421, whereas N-terminal tr-tau was the most abundant form in our study [8,41]. In summary, the finding that a large population of neurons with pathological tau is not detected with common p-tau antibodies is probably highly relevant for understanding AD and PiD pathology. As a start, it reveals a neglected area of investigation related to selective vulnerability and pathogenesis of AD and, to a lesser extent, PiD because almost all studies probe p-tau alone. Also, our study supports the notion that therapeutic approaches for modulating the generation of tr-tau species, including the use of aCasp-6 inhibitors or mAbD13, may be necessary to treat AD in addition to strategies aimed at modulating the accumulation of p-tau species.

Fourth, although most aCasp-6 positive neurons also show positivity for tr-tau, the opposite is not true. As we used validated monoclonal antibodies, it is unlikely that our IF reactions detected tr-tau forms other than D13 and D402. Positivity for aCasp-6 may be a relatively ephemeral process. Thus, the tr-tau forms remain even when aCasp-6 is not present anymore. aCasp-6 predominantly triggers cleavage of tau at D13 and D402. However, another effector Casps, such as Casp-3, Casp-7 or Casp-8, may cleave tau at the D402 and D13 sites. To address this possibility, we performed immunostaining in AD tissue using antibodies against Casp-3. However, we found no positivity for Casp-3 (not shown here because results are negative), in line with other studies failing to identify Casp-3 activation in human brain tissue, possibly due to its very transient nature [16,42,43]. Further studies testing Casp-7 and Casp-8 activity in tauopathies are warranted.

Fifth, D13 and D402 tr-tau were also present in p-tau-positive astroglia in PSP and, to a much lesser extent, CBD, confirming that Casp-mediated tau pathological changes extend beyond neurons in tauopathies (Figure 6; Table S3), in line with previous findings using the mAbTauC3 (D421) [8].

Our approach offers several strengths to maximise analytical rigour. We generated neopeptide mAbs against Casp-6-tr-tau at D402

(C-terminus) and D13 (N-terminus) truncation sites. We also investigated the burden of these inclusions simultaneously with p-tau and aCasp-6 burden in distinct human tauopathies. Our results highlight the importance of studies comparing different tauopathies side by side, as similarities and differences may inform their pathogenesis. When comparing the percentages of neuronal D402 and D13 tr-tau to those of neuronal p-tau in the same disease, the differences between AD/PiD and PSP/CBD become even more apparent. Multiplex IF methods have been limited by difficulties in eluting any antibody, including tau antibodies, while maintaining tissue integrity to allow multiple staining cycles in the same histological slide. Here, we applied a pipeline recently developed in-house that provides excellent elution of tau antibodies verified by rigorous quality control steps [27]. Our methodology enabled us to examine three tau antibodies raised in the same species, simultaneously. Additionally, the simultaneous use of several antibodies in the same tissue section increases confidence in our results. We ran the experiments in a calibrated autostainer to avoid potential biases caused by immunostaining batch variation. This approach also minimises the chances of false-negative results. For instance, all our tissue samples, except for AGD, which is not expected to show p-tau positivity in the MFG [44,45], showed relatively strong p-tau positivity. CBD showed minimal Casp-6 activation compared to the other tauopathies (Table 2; Figures 4 and 5). Finally, we quantified neurons and pathological inclusions in two separate sets of slides of the same case cases, with similar results. Nevertheless, our approach is not free of limitations, many inherent to post-mortem studies involving the human brain. Such limitations include the cross-sectional nature of the specimens and the relatively small number of cases analysed. Obtaining well-characterised post-mortem human brain tissue from healthy controls and rare tauopathies, especially those from cases lacking neuropathological comorbidities, is challenging. Despite our relatively small cohort size, we counted over 56,000 individual neurons in MFG and ITG combined.

In summary, this study demonstrates a strong association between aCasp-6 and tr-tau, suggesting that Casp-6-cleavage of tau in neurons is likely a feature of tauopathies with predominant 3R, rather than 4R, tau. In AD and PiD, sizeable percentages of neurons positive for tr-tau lacked evidence of p-tau. Considering the progressive nature of AD and other tauopathies, early modulation of Casp-6 activation and Casp cleavage of tau could have a significant therapeutic value against tau aggregation and neuronal death. This study further supports the potential of biofluid biomarkers for tr-tau forms to diagnose AD and differentiate AD from other tauopathies at the single patient level. Future studies in human and clinically relevant models of tau pathology, such as iPSCs from patients with MAPT mutations [46], are crucial for a better understanding of caspase-mediated pathways that lead to tau pathology in tauopathies.

ACKNOWLEDGEMENTS

We thank the patients and their families for their invaluable contribution to brain ageing neurodegenerative disease research. We thank Dr. Andrea LeBlanc for helpful discussions on caspase biochemistry and Dr. Peter Davies (Albert Einstein College of Medicine, New York,

NY) for generously providing tau antibodies. This study was supported by the National Institutes of Health K01AG053433 (P.T.); K24AG053435, R56AG057528 and U54 NS100717 (L.T.G.); K08AG052648 (S.S.); P30AG062422 and P01AG019724 (B.L.M.); UCSF RAP Pilot Award programme (P.T.); UCSF RAP Team Science Grant (L.T.G. and M.R.A.); Alzheimer's Association AARG-16-441514 (L.T.G. and M.R.A.), Rainwater Charitable Foundation (M.R.A.); and a Catalyst award from ShangPharma Innovation (M.R.A., T.Y., S. K, R.N.).

CONFLICT OF INTEREST

M.R.A. is cofounder of Elgia Therapeutics, which is developing caspase-6 inhibitors for fibrotic diseases. The other authors have declared no conflict of interest. S.S. received compensation for consulting work with Precision Xtract and Acel Health. A.J.E. received compensation for consulting work with Epiodyne, Inc., 2018. ChemPartner is a Contract Research Organization and has no rights to the antibodies or data.

AUTHOR CONTRIBUTIONS

P.T., A.M.H.P. and L.T.G. designed the study. P.T., A.M.H.P., I.O. and Y.L. performed the experiments, data acquisition and analyses. B.C., T.Y., S.K., R.N., A.J.A. and M.R.A. generated and characterised the neopeptide caspase-cleaved tau antibodies. S.L., A.J.E. and R.A.E. contributed to immunohistochemistry; C.P. and F.L.P. with data analyses and graphic design. S.S., W.W.S., B.L.M. and L.T.G. provided the human brain specimens, P.T. and A.M.H.P. wrote the manuscript. S.S., W.W.S., B.L.M., M.R.A. and L.T.G. revised the manuscript. L.T.G. and M.R.A. supervised the study. F.P. ran the statistical analysis. All authors approved the submitted version.

ETHICS STATEMENT

The UCSF institutional review board determined that clinicopathologic studies on de-identified post-mortem tissue samples, like those used here, are exempt from human subject research according to Exemption 45 CFR 46.104(d)(2).

PEER REVIEW


The peer review history for this article is available at <https://publons.com/publon/10.1111/nan.12819>.

DATA AVAILABILITY STATEMENT

The data that support the findings of this study are available from the corresponding author upon reasonable request.

ORCID

Panos Theofilas  <https://orcid.org/0000-0001-9701-1352>

Alexander J. Ehrenberg  <https://orcid.org/0000-0003-4334-9424>

Michelle R. Arkin  <https://orcid.org/0000-0002-9366-6770>

Lea T. Grinberg  <https://orcid.org/0000-0002-6809-0618>

REFERENCES

- Spillantini MG, Goedert M. Tau pathology and neurodegeneration. *Lancet Neurol.* 2013;12(6):609-622. doi:[10.1016/S1474-4422\(13\)70090-5](https://doi.org/10.1016/S1474-4422(13)70090-5)

2. Rösler TW, Tayaranian Marvian A, Brendel M, et al. Four-repeat tauopathies. *Prog Neurobiol*. 2019;180:101644. doi:10.1016/j.pneurobio.2019.101644
3. Cairns NJ, Bigio EH, Mackenzie IRA, et al. Neuropathologic diagnostic and nosologic criteria for frontotemporal lobar degeneration: consensus of the Consortium for Frontotemporal Lobar Degeneration. *Acta Neuropathol (Berl)*. 2007;114(1):5-22. doi:10.1007/s00401-007-0237-2
4. Morris M, Maeda S, Vossel K, Mucke L. The many faces of tau. *Neuron*. 2011;70(3):410-426. doi:10.1016/j.neuron.2011.04.009
5. Tracy T, Claiborn KC, Gan L. Regulation of tau homeostasis and toxicity by acetylation. *Adv Exp Med Biol*. 2019;1184:47-55. doi:10.1007/978-981-32-9358-8_4
6. Wesseling H, Mair W, Kumar M, et al. Tau PTM profiles identify patient heterogeneity and stages of Alzheimer's disease. *Cell*. 2020;183(6):1699-1713.e13. doi:10.1016/j.cell.2020.10.029
7. de Calignon A, Fox LM, Pitstick R, et al. Caspase activation precedes and leads to tangles. *Nature*. 2010;464(7292):1201-1204. doi:10.1038/nature08890
8. Ferrer I, Lopez-Gonzalez I, Carmona M, et al. Glial and neuronal tau pathology in tauopathies: characterization of disease-specific phenotypes and tau pathology progression. *J Neuropathol Exp Neurol*. 2014;73(1):17-97. doi:10.1097/NEN.0000000000000030
9. Gambin TC, Chen F, Zambrano A, et al. Caspase cleavage of tau: linking amyloid and neurofibrillary tangles in Alzheimer's disease. *Proc Natl Acad Sci U S A*. 2003;100(17):10032-10037. doi:10.1073/pnas.1630428100
10. Zhao Y, Tseng I-C, Heyser CJ, et al. Apoptosis-mediated caspase cleavage of tau contributes to progressive supranuclear palsy pathogenesis. *Neuron*. 2015;87(5):963-975. doi:10.1016/j.neuron.2015.08.020
11. Gray DC, Mahrus S, Wells JA. Activation of specific apoptotic caspases with an engineered small-molecule-activated protease. *Cell*. 2010;142(4):637-646. doi:10.1016/j.cell.2010.07.014
12. Hyman BT, Yuan J. Apoptotic and non-apoptotic roles of caspases in neuronal physiology and pathophysiology. *Nat Rev Neurosci*. 2012;13(6):395-406. doi:10.1038/nrn3228
13. Dagbay KB, Hardy JA. Multiple proteolytic events in caspase-6 self-activation impact conformations of discrete structural regions. *Proc Natl Acad Sci National Academy of Sciences*. 2017;114(38):E7977-E7986. doi:10.1073/pnas.1704640114
14. Klaiman G, Champagne N, LeBlanc AC. Self-activation of Caspase-6 in vitro and in vivo: Caspase-6 activation does not induce cell death in HEK293T cells. *Biochim Biophys Acta*. 2009;1793(3):592-601. doi:10.1016/j.bbamcr.2008.12.004
15. Albrecht S, Bourdeau M, Bennett D, Mufson EJ, Bhattacharjee M, LeBlanc AC. Activation of caspase-6 in aging and mild cognitive impairment. *Am J Pathol*. 2007;170(4):1200-1209. doi:10.2353/ajpath.2007.060974
16. Guo H, Albrecht S, Bourdeau M, Petzke T, Bergeron C, LeBlanc AC. Active caspase-6 and caspase-6-cleaved tau in neuropil threads, neuritic plaques, and neurofibrillary tangles of Alzheimers disease. *Am J Pathol*. 2004;165(2):523-531. doi:10.1016/S0002-9440(10)63317-2
17. Theofilas P, Ehrenberg AJ, Nguy A, et al. Probing the correlation of neuronal loss, neurofibrillary tangles, and cell death markers across the Alzheimers disease Braak stages: a quantitative study in humans. *Neurobiol Aging*. 2018;61:1-12. doi:10.1016/j.neurobiolaging.2017.09.007
18. Foveau B, Albrecht S, Bennett DA, Correa JA, LeBlanc AC. Increased Caspase-6 activity in the human anterior olfactory nuclei of the olfactory bulb is associated with cognitive impairment. *Acta Neuropathol Commun*. 2016;4(1):127. doi:10.1186/s40478-016-0400-x
19. Horowitz PM, Patterson KR, Guillozet-Bongaarts AL, et al. Early N-terminal changes and caspase-6 cleavage of tau in Alzheimers disease. *J Neurosci off J Soc Neurosci*. 2004;24(36):7895-7902. doi:10.1523/JNEUROSCI.1988-04.2004
20. Ramcharitar J, Albrecht S, Afonso VM, Kaushal V, Bennett DA, LeBlanc AC. Cerebrospinal fluid tau cleaved by caspase-6 reflects brain levels and cognition in aging and Alzheimer disease. *J Neuropathol Exp Neurol*. 2013;72(9):824-832. doi:10.1097/NEN.0b013e3182a0a39f
21. Eser RA, Ehrenberg AJ, Petersen C, et al. Selective vulnerability of brainstem nuclei in distinct tauopathies: a postmortem study. *J Neuropathol Exp Neurol*. 2018;77(2):149-161. doi:10.1093/jnen/nlx113
22. Montine TJ, Phelps CH, Beach TG, et al. National Institute on Aging-Alzheimer's Association guidelines for the neuropathologic assessment of Alzheimers disease: a practical approach. *Acta Neuropathol (Berl)*. 2012;123(1):1-11. doi:10.1007/s00401-011-0910-3
23. Mackenzie IRA, Neumann M, Bigio EH, et al. Nomenclature and nosology for neuropathologic subtypes of frontotemporal lobar degeneration: an update. *Acta Neuropathol (Berl)*. 2010;119(1):1-4. doi:10.1007/s00401-009-0612-2
24. Theofilas P, Wang C, Butler D, et al. Caspase inhibition mitigates tau cleavage and neurotoxicity in iPSC-induced neurons with the V337M MAPT mutation. *bioRxiv*. 2021;425912.
25. Arai T, Ikeda K, Akiyama H, et al. Different immunoreactivities of the microtubule-binding region of tau and its molecular basis in brains from patients with Alzheimers disease, Picks disease, progressive supranuclear palsy and corticobasal degeneration. *Acta Neuropathol (Berl)*. 2003;105(5):489-498. doi:10.1007/s00401-003-0671-8
26. Su JH, Cummings BJ, Cotman CW. Early phosphorylation of tau in Alzheimers disease occurs at Ser-202 and is preferentially located within neurites. *Neuroreport*. 1994;5(17):2358-2362. doi:10.1097/00001756-199411000-00037
27. Ehrenberg AJ, Morales DO, Piergies AMH, et al. A manual multiplex immunofluorescence method for investigating neurodegenerative diseases. *J Neurosci Methods*. 2020;339:108708. doi:10.1016/j.jneumeth.2020.108708
28. Braak H, Braak E. Neuropathological staging of Alzheimer-related changes. *Acta Neuropathol (Berl)*. 1991;82(4):239-259. doi:10.1007/BF00308809
29. Coughlin DG, Dickson DW, Josephs KA, Litvan I. Progressive supranuclear palsy and corticobasal degeneration. *Adv Exp Med Biol*. 2021;1281:151-176. doi:10.1007/978-3-030-51140-1_11
30. Karikari TK, Pascoal TA, Ashton NJ, et al. Blood phosphorylated tau 181 as a biomarker for Alzheimers disease: a diagnostic performance and prediction modelling study using data from four prospective cohorts. *Lancet Neurol*. 2020;19(5):422-433. doi:10.1016/S1474-4422(20)30071-5
31. Cicognola C, Brinkmalm G, Wahlgren J, et al. Novel tau fragments in cerebrospinal fluid: relation to tangle pathology and cognitive decline in Alzheimers disease. *Acta Neuropathol (Berl)*. 2019;137(2):279-296. doi:10.1007/s00401-018-1948-2
32. Sato C, Barthélemy NR, Mawuenyega KG, et al. Tau kinetics in neurons and the human central nervous system. *Neuron*. 2018;97(6):1284-1298. doi:10.1016/j.neuron.2018.02.015
33. Chen Z, Mengel D, Keshavan A, et al. Learnings about the complexity of extracellular tau aid development of a blood-based screen for Alzheimer's disease. *Alzheimers Dement J Alzheimers Assoc*. 2019;15(3):487-496. doi:10.1016/j.jalz.2018.09.010
34. Chhatwal JP, Schultz AP, Dang Y, et al. Plasma N-terminal tau fragment levels predict future cognitive decline and neurodegeneration in healthy elderly individuals. *Nat Commun Nature Publishing Group*. 2020;11:6024.
35. Mengel D, Janelidze S, Glynn RJ, Liu W, Hansson O, Walsh DM. Plasma NT1 tau is a specific and early marker of Alzheimer's disease. *Ann Neurol*. 2020;88(5):878-892. doi:10.1002/ana.25885

36. Guillozet-Bongaarts AL, Glajch KE, Libson EG, et al. Phosphorylation and cleavage of tau in non-AD tauopathies. *Acta Neuropathol (Berl)*. 2007;113(5):513-520. doi:[10.1007/s00401-007-0209-6](https://doi.org/10.1007/s00401-007-0209-6)
37. Cho J-H, Johnson GVW. Glycogen synthase kinase 3 beta induces caspase-cleaved tau aggregation in situ. *J Biol Chem*. 2004;279(52):54716-54723. doi:[10.1074/jbc.M403364200](https://doi.org/10.1074/jbc.M403364200)
38. Canu N, Dus L, Barbato C, et al. Tau cleavage and dephosphorylation in cerebellar granule neurons undergoing apoptosis. *J Neurosci off J Soc Neurosci UNITED STATES*. 1998;18(18):7061-7074. doi:[10.1523/JNEUROSCI.18-18-07061.1998](https://doi.org/10.1523/JNEUROSCI.18-18-07061.1998)
39. Delobel P, Lavenir I, Fraser G, et al. Analysis of tau phosphorylation and truncation in a mouse model of human tauopathy. *Am J Pathol Elsevier*. 2008;172(1):123-131. doi:[10.2353/ajpath.2008.070627](https://doi.org/10.2353/ajpath.2008.070627)
40. Rissman RA, Poon WW, Blurton-Jones M, et al. Caspase-cleavage of tau is an early event in Alzheimer disease tangle pathology. *J Clin Invest*. 2004;114(1):121-130. doi:[10.1172/JCI200420640](https://doi.org/10.1172/JCI200420640)
41. Flores-Rodríguez P, Ontiveros-Torres MA, Cárdenas-Aguayo MC, et al. The relationship between truncation and phosphorylation at the C-terminus of tau protein in the paired helical filaments of Alzheimers disease. *Front Neurosci*. 2015;9:33. doi:[10.3389/fnins.2015.00033](https://doi.org/10.3389/fnins.2015.00033)
42. LeBlanc A, Liu H, Goodyer C, Bergeron C, Hammond J. Caspase-6 role in apoptosis of human neurons, amyloidogenesis, and Alzheimers disease. *J Biol Chem*. 1999;274(33):23426-23436. doi:[10.1074/jbc.274.33.23426](https://doi.org/10.1074/jbc.274.33.23426)
43. Selznick LA, Holtzman DM, Han BH, et al. In situ immunodetection of neuronal caspase-3 activation in Alzheimer disease. *J Neuropathol Exp Neurol*. 1999;58(9):1020-1026. doi:[10.1097/00005072-199909000-00012](https://doi.org/10.1097/00005072-199909000-00012)
44. Grinberg LT, Heinsen H. Argyrophilic grain disease: an update about a frequent cause of dementia. *Dement Neuropsychol*. 2009;3(1):2-7. doi:[10.1590/S1980-57642009DN30100002](https://doi.org/10.1590/S1980-57642009DN30100002)
45. Kovacs GG. Invited review: Neuropathology of tauopathies: principles and practice. *Neuropathol Appl Neurobiol* John Wiley & Sons, Ltd. 2015;41(1):3-23. doi:[10.1111/nan.12208](https://doi.org/10.1111/nan.12208)
46. Karch CM, Kao AW, Karydas A, et al. A comprehensive resource for induced pluripotent stem cells from patients with primary tauopathies. *Stem Cell Rep*. 2019;13(5):939-955. doi:[10.1016/j.stemcr.2019.09.006](https://doi.org/10.1016/j.stemcr.2019.09.006)

SUPPORTING INFORMATION

Additional supporting information may be found in the online version of the article at the publisher's website.

How to cite this article: Theofilas P, Piergies AMH, Oh I, et al. Caspase-6-cleaved tau is relevant in Alzheimer's disease and marginal in four-repeat tauopathies: Diagnostic and therapeutic implications. *Neuropathol Appl Neurobiol*. 2022; e12819. doi:[10.1111/nan.12819](https://doi.org/10.1111/nan.12819)